

# Observations of ultraslow light-based photon logic gates: NAND/OR

B. S. Ham<sup>a)</sup> and J. Hahn

Center for Photon Information Processing and the Graduate School of Information and Telecommunications, Inha University, 253 Yonghyun-dong, Nam-gu, Incheon 402-751, Republic of Korea

(Received 14 October 2008; accepted 21 February 2009; published online 12 March 2009)

We report observations of photon logic gate operations using ultraslow light phenomena in a rare-earth doped solid medium. Unlike conventional optical logic gates based on semiconductor optical amplifiers, the present photon logic gate utilizes spin coherence, which is completely free from the optical population constraint and gives potential for ultrahigh speed operations. In addition to the possibility of ultralow power operations, the usage of ultraslow light gives a benefit of all-optical buffer memory functions. Thus, the present demonstration has potential applications to cascable photon logic devices. © 2009 American Institute of Physics. [DOI: 10.1063/1.3099039]

Light control by another light has been intensively studied for the past two decades. Recently refractive index control of an optical medium has been demonstrated for potential applications of using ultraslow light phenomena.<sup>1–10</sup> Electromagnetically induced transparency<sup>11</sup> (EIT) has been applied to induce a narrow transparency window in an absorption spectrum, where the absorption spectrum correlates with a dispersion line shape by Kramers–Kronig relation.<sup>12</sup> The ultraslow light resulting from a steep dispersion line shape offers potential applications to all-optical information processing, such as optical buffer memories<sup>5</sup> and photon routers,<sup>7</sup> as well as quantum information processing such as entanglement generations<sup>9</sup> and quantum memories.<sup>2,10</sup>

Nondegenerate four-wave mixing generations based on EIT have been intensively studied for efficient nonlinear optics owing to absorption reduction resulting from destructive quantum interference at even resonance frequency, while keeping maximum nonlinear coefficient.<sup>13–16</sup> The physics of nondegenerate four-wave mixing processing also has been investigated for coherence conversion process between the spin coherence and the four-wave mixing signal.<sup>17</sup> In a non-slow light regime, ultrahigh speed quantum switching has been observed, where the switching time is two orders of magnitude shorter than the optical population relaxation time,<sup>18</sup> which is a constraint of most conventional optical switching technologies. The ultraslow light-based optical switching<sup>7</sup>—so-called photon routing—gives the same benefit of ultrahigh speed switching as in the quantum switching method<sup>18</sup> with an additional benefit of all-optical buffer memory functions owing to the ultralong group delay.

Photon routing is a quantum mechanical phenomenon based on quantum coherence and is free from both population relaxation constraint and size-dependent switching speed.<sup>7</sup> The size-dependent switching speed becomes a critical issue in modern electronic technologies such as CPUs and memories governed by Moore's law. Thus, the present research may provide a solution to the size and speed limitations of modern electronic technologies, because ultraslow light-based photon routing can be sustained for a single photon regime interacting with an atomic (ionic) ensemble whose physical size is diffraction limited.<sup>18</sup> In this letter, we

present all-optical logic gate operations as a proof of principle for the ultrahigh speed photon devices, using a pair of independent optical nodes, where each node utilizes ultraslow light-based photon routing. For potential applications of ultrahigh speed logic gates, an ultrafast decaying medium such as semiconductor quantum wells might be a good candidate, where EIT has been demonstrated already,<sup>19</sup> and hyperterahertz photon switching has been suggested.<sup>20</sup> We experimentally demonstrate Boolean logic gates of NAND and OR simultaneously in the same unit. For this demonstration, we use a rare-earth Pr<sup>3+</sup> doped Y<sub>2</sub>SiO<sub>5</sub> (Pr:YSO) as an optical medium at a cryogenic temperature of ~5 K. The size of the optical medium of Pr:SYO is 4(H) × 5(W) × 5(L) mm<sup>3</sup>.

Figure 1 shows a schematic diagram of photon logic gates, NAND and OR, based on a set of parallel photon routers. Each photon router in Fig. 1(a) satisfies the energy level diagram in Fig. 1(b), where the input P is an optical signal coming in from both photon routers simultaneously. The signals A1 and A2, respectively, act as logic inputs for logic outputs S and D and S' and D'. Here, the diffraction signal D (D') results from slow-light-enhanced nondegenerate four-wave mixing processes: photon routing.<sup>7</sup> The detuning  $\Delta$  in Fig. 1(b) is set to 1 MHz to avoid any unnecessary argument of standing wave gratings. To satisfy the slow light condition, the control field C covers both P and A, as shown in Fig. 1(c). The temporal position of the logic input A (A') coincides with the slow light S (S'). The optical depth  $d$  of

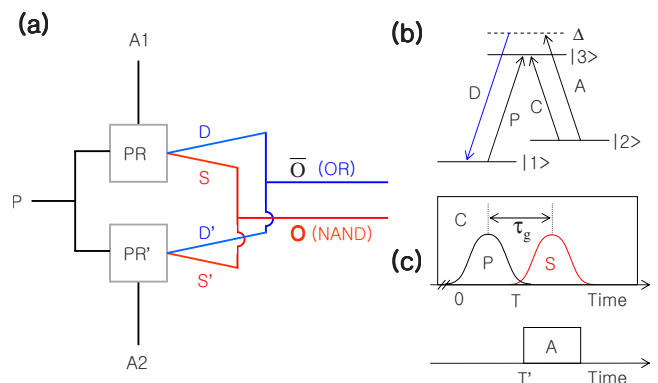


FIG. 1. (Color online) Schematic of photon logic gate. (a) Block diagram of a photon logic gate using a set of parallel photon routers. (b) Energy level diagram of nondegenerate four-wave mixing processes. (c) Pulse sequence.

<sup>a)</sup> Author to whom correspondence should be addressed. Electronic mail: bham@inha.ac.kr.

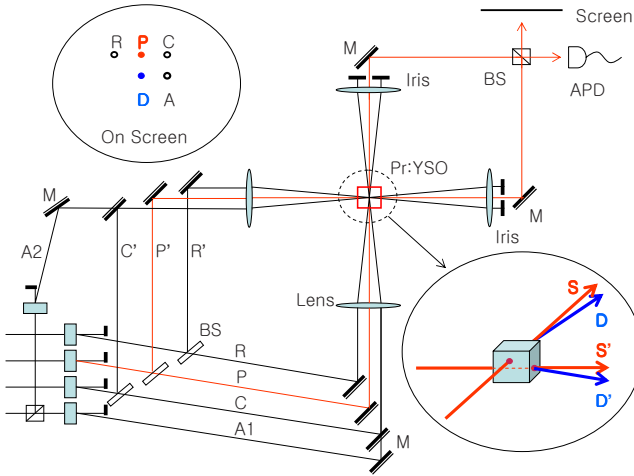


FIG. 2. (Color online) Experimental setup of photon logic gate: M denotes mirror, BS denotes beam splitter and APD denotes avalanche photodiode.

the probe light  $P$  is  $\sim 10: d = \alpha l$ , where  $\alpha$  is an absorption coefficient and  $l$  is the propagation length of the medium. The absorption coefficient  $\alpha$  is  $N$  dependent, where  $N$  is the density of atoms interacting with the probe  $P$  to determine the optical depth  $d$  (Ref. 1)

$$\tau_g \propto \frac{\Omega_C}{N}. \quad (1)$$

Thus, the group delay  $\tau_g$  is controllable with the coupling/repump light intensities and can be used for the function of all-optical buffer memory.

Figure 2 shows a schematic of experimental setup for the photon logic gates. The total of four laser inputs is generated from a single ring-dye laser output. The probe field  $P$  is a Gaussian pulse, and others ( $R$ ,  $C$ , and  $A$ ) are square pulses. The light beam  $R$  whose pulse length is 10 ms, precedes the coupling  $C$  by 200  $\mu$ s and acts as a repump to prepare the same optical depth for the probe  $P$ ; otherwise the inherent persistent spectral hole-burning phenomenon of the Pr:YSO depletes all atoms from both states  $|1\rangle$  and  $|2\rangle$  to the third state [not shown in Fig. 1(b)].<sup>21</sup> The pulse train of Fig. 1(c) is repeated at 20 Hz. To provide independent optical nodes for photon routers shown in Fig. 1(a), the set of laser beams ( $R$ ,  $A$ ,  $C$ , and  $P$ ) is split into two groups, and each group is used to focus into the sample at different locations (optical nodes) separated by  $\sim 1$  mm, as shown in the lower inset of Fig. 2. The power of  $R$  ( $R'$ ),  $C$  ( $C'$ ),  $A1$  ( $A2$ ), and  $P$  ( $P'$ ) is 1.5 (1.6), 12.8 (11.7), 11.5 (12.4), and 0.46 (0.52) mW. Both outputs are combined by a beam splitter and sent to an avalanche photodiode. In Fig. 2, only a slow light ( $S$ ) detection scheme is shown. The detected signals are averaged for 30 trials and recorded for  $S$  ( $S'$ ) and  $D$  ( $D'$ ) simultaneously. The upper left inset shows spatial layout of the beams on the screen by opening the last iris after passing through the

sample. As shown, the nondegenerate four-wave mixing signal  $D$  ( $D'$ ) satisfies the phase matching condition:  $\mathbf{k}_D = \mathbf{k}_P - \mathbf{k}_C + \mathbf{k}_A$ . On the surface of the focusing lens ( $f=40$  cm) all beams are separated by  $\sim 5$  mm generating overall  $\sim 80\%$  overlap through the medium.

With combinations of both logic inputs  $A1$  and  $A2$  in Fig. 1(a), we set a truth table of Boolean logic (NAND and OR) in Table I (see Ref. 7 for the detail functions of PR). Under  $C$ , the input signal  $P$  turns into  $S$ . If  $A1$  ( $A2$ ) applies to PR ( $PR'$ ) for  $S$ , then  $S$  switches into  $D$ .<sup>7</sup> Thus,  $S$  ( $S'$ ) exists if and only if there is no control logic input. Outputs  $S$  ( $D$ ) and  $S'$  ( $D'$ ) are added together to form logic output  $O$  ( $S+S'$ ) for NAND and  $\bar{O}$  ( $D+D'$ ) for OR.

Experimental results of the photon logic operations are presented in Fig. 3(a). The top red-colored curve represents slow light pulses  $S$  resulting from four consecutive input  $P$  pulses (1 1 1 1) separated by  $T=400$   $\mu$ s. Here, “1” (“0”) stands for “ON” (“OFF”). The preceding small bump of each slow light  $S$  is  $P$  residual.<sup>2,7</sup> The second (orange) and third (green) curves are the logic inputs  $A1$  (1 1 0 0) and  $A2$  (0 1 0 1), respectively. The fourth (blue) and fifth (purple) curves are the logic outputs  $O$  (1 0 1 1) and  $\bar{O}$  (1 1 0 1), respectively. The reason for the bigger intensity of each output for  $O$  and  $\bar{O}$  at  $t=1500$   $\mu$ s and  $t=1100$   $\mu$ s, respectively, is due to the addition of signals as mentioned. Thus, the Boolean logic gates, NAND ( $O$ ) and OR ( $\bar{O}$ ) in Table I are experimentally proven. The observed photon logic gates imply two important functions: (1) all-optical gating (switching/routing) and (2) all-optical buffer memory. Considering that an active node size is diffraction limited, the present photon logic gate can be applied to a microphoton device as a scalable building block, as a transistor is applied to electronic logic gates (see resistor-transistor-logic).

As supplemental data, photon routing and EIT are presented in Figs. 3(c) and 3(d), respectively. Figure 3(c) is an extended version of the dotted region of Fig. 3(a). The spectral width of the EIT window used in Fig. 3(a) is  $\sim 100$  kHz and is shown in Fig. 3(d). Here, the conversion efficiency of the enhanced nondegenerate four-wave mixing signal  $D$  in Fig. 3(c) is much higher than that in a nonslow light regime<sup>13,14,18</sup> owing to slow-light-enhanced spin coherence<sup>7</sup>

$$I_D \propto I_A [\text{Re}(\rho_{12})]^2, \quad (2)$$

where  $\rho_{12}$  is the resonant Raman field ( $P$  and  $C$ )-excited spin coherence, and  $I_i$  is an intensity of the field  $i$ . The measured conversion efficiency (intensity ratio of  $D$  to  $S$ ) in Fig. 3(a) [and also in Fig. 3(c)] is  $\sim 270\%$ . Considering the optical depth  $d \sim 10$  and the nonperfect overlap condition, the obtained conversion efficiency in Fig. 3 is extremely high. This provides a direct proof of the slow-light-enhanced nondegenerate four-wave mixing processes, and potential applications of the present photon logic gates. Unlike photon-echo-based,<sup>22</sup> this amplified logic output signal offers

TABLE I. Truth table of Boolean logic NAND and OR for Fig. 3(a). Legends are referred to in Figs. 1 and 2.

P	A1	A2	S	S'	D	D'	$O(S+S')$ :NAND	$\bar{O}(D+D')$ :OR
1	1	0	0	1	1	0	1	1
1	1	1	0	0	0	1	0	1
1	0	0	1	1	0	0	1	0
1	0	1	1	0	0	1	1	1

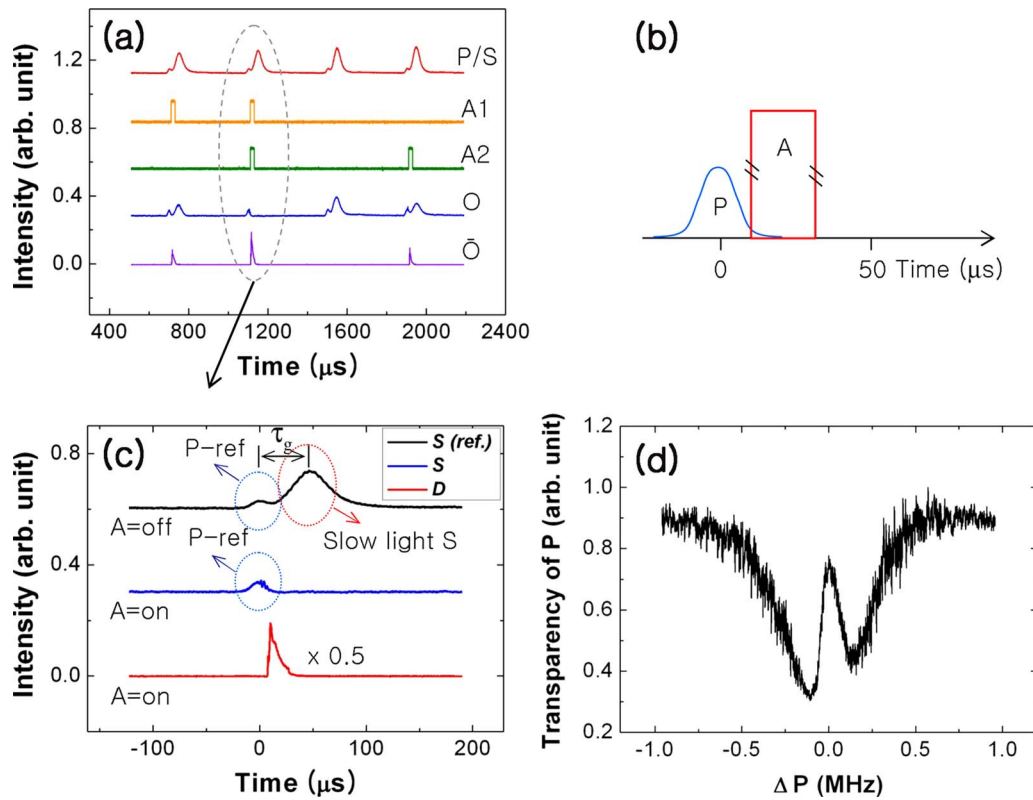


FIG. 3. (Color online) Observations of photon logic gates. (a) Experimental demonstration of ultraslow light-based photon logic gates: NAND and OR. (b) Pulse sequence for photon routing. (c) Ultraslow light-based photon routing. (d) EIT used for (a).  $\Delta P$  stands for detuning from the resonance frequency of P in Fig. 1(b).

great benefit feeding itself into another logic gate as an input signal.

In conclusion, we observed photon logic gate operations of NAND and OR using a pair of photon routers based on ultraslow light-enhanced nondegenerate four-wave mixing processes. The significance of the present observations of the photon logic gate is a demonstration of slow light-based optical logic gate, where the physics is completely different from conventional optical logic gates. The basic physics of the photon logic gates lies in resonant Raman field-excited spin coherence<sup>17</sup> and ultraslow light enhanced nondegenerate four-wave mixing processes. Noting that both the optical population relaxation time and a relatively bigger size (approximately millimeter) are limiting factors in conventional all-optical logic technologies using semiconductor optical amplifiers,<sup>23</sup> the present demonstration has potential for a scalable ultrahigh speed all-optical logic gate whose gating speed is limited by spin dephasing time.<sup>24</sup> In semiconductor quantum structures, whose spin dephasing time is as short as picoseconds, a photonic processor in a hyper-100-GHz regime can be possible even using an extremely low light power owing to the ultraslow light phenomenon.

B.S.H. acknowledges that this work was supported by the Creative Research Initiative Program (Center for Photon Information Processing) of MEST via KOSEF, South Korea.

<sup>1</sup>L. V. Hau, S. E. Harris, Z. Dutton, and C. H. Behroozi, *Nature (London)* **397**, 594 (1999).

- <sup>2</sup>A. V. Turukhin, V. S. Sudarshanam, M. S. Shahriar, J. A. Musser, B. S. Ham, and P. R. Hemmer, *Phys. Rev. Lett.* **88**, 023602 (2002).
- <sup>3</sup>M. S. Bigelow, N. N. Lepeshkin, and R. W. Boyd, *Science* **301**, 200 (2003).
- <sup>4</sup>P.-C. Ku, F. Sedgwick, C. Chang-Hasnain, J. Connie, P. Palinginis, T. Li, and H. Wang, *Opt. Lett.* **29**, 2291 (2004).
- <sup>5</sup>F. Xia, L. Sekaric, and L. Vlasov, *Nat. Photonics* **1**, 65 (2006).
- <sup>6</sup>A. Andre, M. Bajcsy, A. S. Zibrov, and M. D. Lukin, *Phys. Rev. Lett.* **94**, 063902 (2005).
- <sup>7</sup>B. S. Ham, *Phys. Rev. A* **78**, 011808(R) (2008).
- <sup>8</sup>S. A. Moiseev and B. S. Ham, *Phys. Rev. A* **71**, 053802 (2005).
- <sup>9</sup>M. D. Lukin and A. Imamoglu, *Phys. Rev. Lett.* **84**, 1419 (2000).
- <sup>10</sup>C. Liu, Z. Dutton, C. H. Behroozi, and L. V. Hau, *Nature (London)* **409**, 490 (2001).
- <sup>11</sup>S. E. Harris, *Phys. Today* **50**, 36 (1997).
- <sup>12</sup>R. W. Boyd, *Nonlinear Optics*, 3rd ed. (Academic, New York, 2008).
- <sup>13</sup>Y.-Q. Li and M. Xiao, *Opt. Lett.* **21**, 1064 (1996).
- <sup>14</sup>B. S. Ham, M. S. Shahriar, and P. R. Hemmer, *Opt. Lett.* **22**, 1138 (1997).
- <sup>15</sup>S. E. Harris, *Phys. Rev. Lett.* **82**, 4611 (1999).
- <sup>16</sup>L. Deng, M. Kozuma, E. W. Hagley, and M. G. Payne, *Phys. Rev. Lett.* **88**, 143902 (2002).
- <sup>17</sup>B. S. Ham, *Opt. Express* **16**, 5350 (2008).
- <sup>18</sup>B. S. Ham, *Appl. Phys. Lett.* **85**, 893 (2004).
- <sup>19</sup>M. C. Phillips, H. Wang, I. Romyantsev, H. H. Kwong, R. Takayama, and R. Binder, *Phys. Rev. Lett.* **91**, 183602 (2003).
- <sup>20</sup>B. S. Ham, *Appl. Phys. Lett.* **78**, 3382 (2001).
- <sup>21</sup>K. Holliday, M. Croci, E. Vauthey, and U. P. Wild, *Phys. Rev. B* **47**, 14741 (1993).
- <sup>22</sup>S. Kroll and U. Elman, *Opt. Lett.* **18**, 1834 (1993).
- <sup>23</sup>K. E. Stubkjaer, *IEEE J. Sel. Top. Quantum Electron.* **6**, 1428 (2000); J. H. Kim, Y. M. Jhon, Y. T. Byun, S. Lee, D. H. Woo, and S. H. Kim, *IEEE Photonics Technol. Lett.* **14**, 1436 (2002).
- <sup>24</sup>B. S. Ham and P. R. Hemmer, *Phys. Rev. B* **68**, 073102 (2003).